THEMED ISSUE ARTICLE



Check for updates

PDE4D and PDE3B orchestrate distinct cAMP microdomains in 3T3-L1 adipocytes

Johannes Krier^{1,2,3} | David Spähn⁴ | David Arturo Juarez Lopez^{1,2,3} |

Judith L. Nono^{1,2,3} | Judith Seigner^{1,2,3} | Lisa Jacob^{1,2,3} | Siegfried Ussar^{3,5}

Robert Lukowski⁴ | Andreas L. Birkenfeld^{1,2,3} | Gencer Sancar^{1,2,3} ©

²Institute for Diabetes Research and Metabolic Diseases, Helmholtz Center Munich, University of Tübingen, Tübingen, Germany

⁴Institute of Pharmacy, Department of Pharmacology Toxicology and Clinical Pharmacy University of Tübingen, Tübingen, Germany

⁵Research Unit Adipocytes & Metabolism (ADM), Helmholtz Diabetes Center, Helmholtz Center Munich, German Research Center for Environmental Health GmbH, Neuherberg, Germany

Correspondence

Gencer Sancar, Department of Internal Medicine IV, Division of Diabetology, Endocrinology and Nephrology, University of Tübingen, Tübingen, Germany.

Email: gencer.sancar@med.uni-tuebingen.de

Funding information

Deutsche Forschungsgemeinschaft, Grant/Award Numbers: 335549539, 562635405, Bi 1292/ 12-1, LU 1490/10-1; Deutsches Zentrum für Diabetesforschung; German Center for Diabetes Research (DZD)

Abstract

Background and Purpose: Lipolysis is tightly regulated by pro-lipolytic β-adrenoceptor signalling, which activates the cAMP/PKA pathway, and by antilipolytic hormones like insulin and FGF1, which counter-regulate lipolysis through cAMP-degrading phosphodiesterases (PDEs). While the spatial compartmentalization of cAMP signalling is recognized, comparisons between distinct cAMP pools remain under-investigated in adipocytes. Moreover, the dynamics of cAMP around lipid droplets (LD) where lipolysis occurs, are particularly intriguing. Thus, we studied whether adipose FGF1/PDE4D and insulin/PDE3B pathways regulate distinct cAMP microdomains to execute their antilipolytic actions.

Experimental Approach: We evaluated the role of subcellular cAMP pools in lipolysis regulation by PDEs, or antilipolytic hormones, by utilizing EPAC1-based FRET cAMP biosensors specifically designed to localize in the cytoplasm or at the plasma membrane of living cells. Additionally, we developed the first LD-associated cAMP biosensor by fusing the lipid droplet-associated protein perilipin-1 to the EPAC1-based probe.

Key Results: We identified previously unrecognized cAMP pools surrounding LDs that are distinct from cytoplasmic cAMP and resistant to PDE inhibition or antilipolytic stimuli. PDE4D exhibits a stronger effect on all three cAMP pools investigated than PDE3B. FGF1 mainly inhibits the cAMP in the initiation of the signalling at the plasma membrane, whereas insulin targets mainly cytoplasmic cAMP pools.

Conclusion and Implications: The discovery of LD-associated cAMP as a distinct subcellular pool suggests that cAMP signalling in adipocytes is more compartmentalized than previously recognized. The distinct pathways by which FGF1 and insulin regulate adipose cell cAMP levels highlight that antilipolytic signalling is not uniform, refining our understanding of lipolysis regulation.

Abbreviations: adAAV, adipose-specific adeno-associated virus; cAMP, 3',5'-cyclic adenosine monophosphate; CFP, cyan fluorescent protein; FGF1, fibroblast growth factor 1; FRET, Förster resonance energy transfer; HGP, hepatic glucose production; HSL, hormon-sensitive lipase; IBMX, 3'isobutyl'1'methylxanthin; KRBH, Krebs'Ringer bicarbonate HEPES; LD, lipid droplet; NEFA, non'esterified fatty acid; ISO, isoproterenol; PDE, phosphodiesterase; YFP, yellow fluorescent protein.

This is an open access article under the terms of the Creative Commons Attribution License, which permits use, distribution and reproduction in any medium, provided the original work is properly cited.

© 2025 The Author(s). British Journal of Pharmacology published by John Wiley & Sons Ltd on behalf of British Pharmacological Society.

¹Department of Internal Medicine IV, Division of Diabetology, Endocrinology and Nephrology, University of Tübingen, Tübingen, Germany

³German Center for Diabetes Research (DZD), Neuherberg, Germany

onlinelibrary.wiley.com/doi/10.1111/bph.70216 by Helmholtz

Wiley Online Library on [15/10/2025]. See the Terms

Online Library for rules of use; OA

KEYWORDS

cAMP, FGF1, FRET, insulin, lipolysis, PDE3B, PDE4D

1 | INTRODUCTION

Adipocytes store energy as triglycerides (TGs) in lipid droplets (LDs). Lipolysis, the breakdown of TGs, is mainly regulated by 3',5'-cyclic adenosine monophosphate (cAMP)/PKA signalling, which stimulates lipolysis, and cAMP-hydrolyzing phosphodiesterases (PDEs), which counteract it. During fasting, catecholamines activate β-adrenoceptors, stimulating adenylyl cyclases to convert ATP into cAMP. Elevated cAMP activates PKA, which phosphorylates key lipolytic proteins, including hormone-sensitive lipase (HSL) and LDassociated protein perilipin 1, facilitating HSL recruitment to LDs. HSL then hydrolyzes TGs into diacylglycerols and monoglycerides, releasing non-esterified fatty acids (NEFAs) and glycerol, which can be used for ATP production. Additionally, adipose TG lipase plays a crucial role by hydrolyzing TGs into diacylglycerols, further enhancing the lipolytic process. In vivo, released NEFAs and glycerol from adipocytes contribute to hepatic glucose production (HGP) during fasting. In the healthy state, postprandial insulin efficiently suppresses HPG by directly promoting glycogen synthesis in the liver and indirectly reducing lipolysis through downregulation of the cAMP/PKA pathway. thereby further lowering HGP (Perry et al., 2015; Petersen et al., 2017). In Type 2 diabetes, the suppression of lipolysis and HGP is impaired, contributing to hyperglycemia (Sharabi et al., 2015). Moreover, uncontrolled lipolysis is also associated with lipotoxicity in other organs and exacerbates insulin resistance (Boesch et al., 2024; Gerst et al., 2019; Sancar & Birkenfeld, 2024; Sárvári et al., 2021). Hence, understanding how lipolysis is regulated remains of high importance to manage insulin resistance in Type 2 diabetes.

While the cAMP/PKA pathway is well established as the primary driver of lipolysis, more recent findings suggest that cAMP signalling is compartmentalized into microdomains within adipocytes, leading to localized regulation of PKA activity (De Jong et al., 2023, 2025; Kannabiran et al., 2020; Zhang et al., 2005). These cAMP microdomains are defined by a balance between adenylyl cyclases, PDEs and A-kinase anchoring proteins, which tether PKA to specific cellular structures, potentially including LDs (Ahmad et al., 2015). PDEs, particularly PDE3B and PDE4 isoforms, play a crucial role in shaping local cAMP levels and regulating lipolysis (Choi et al., 2006; DiPilato et al., 2015; Nakamura et al., 2004; Sancar et al., 2022). PDE3B, activated by insulin degrades cAMP, reducing PKA activity and thereby inhibiting lipolysis. Conversely, PDE4D is thought to modulate lipolysis under basal and catecholamine-stimulated conditions and does not significantly contribute to the antilipolytic role of insulin at least in insulin-sensitive states (Enoksson et al., 1998; Hagström-Toft et al., 1995; Wang & Edens, 2007). Previously, we showed that Fibroblast growth factor 1 (FGF1) activates PDE4D antilipolytic activity via phosphorylation of a crucial residue that serves as a priming site (Gasser et al., 2022; Sancar et al., 2022). While PDE3 and PDE4

What is already known?

- Lipolysis is regulated by β -adrenergic signalling and antilipolytic hormones insulin and FGF1 through phosphodiesterases.
- cAMP signalling is spatially compartmentalized within cells, allowing localized regulation of cellular processes.

What does this study add?

- Discovery of a distinct cAMP pool surrounding lipid droplets, separate from cytoplasmic cAMP.
- Identified that FGF1 selectively inhibits plasma membrane cAMP, whereas insulin targets cytoplasmic cAMP.

What is the clinical significance?

- Distinct cAMP pools regulated by FGF1 and insulin offer novel targets to modulate lipolysis.
- Targeting specific cAMP compartments or PDE isoforms may improve insulin resistance therapies.

activity compromises the main PDE activity in adipocytes, their relative contribution to subcellular cAMP pools remains unidentified (Choi et al., 2006). Recent studies indicated differential regulation of cAMP microdomains by different β -adrenoceptor subtypes in adipocytes (De Jong et al., 2023). Moreover, induction of insulin resistance shifts the main PDE activity from PDE3 to PDE4 in human adipocytes (De Jong et al., 2023). Despite growing evidence that cAMP pools are spatially restricted, how these local pools specifically influence lipolysis remains poorly understood. It is also unknown whether cAMP microdomains exist at the LD surface and, if so, whether they are differentially regulated by PDEs and/or antilipolytic hormones such as insulin or FGF-1. Additionally, the contribution of PDE3B or PDE4D within these microdomains is unknown, raising the possibility that distinct PDEs regulate different cAMP microdomains.

In the current study, we employed subcellular targeted Förster resonance energy transfer (FRET)-based cAMP biosensors to investigate the cAMP changes surrounding the plasma membrane, cytoplasm and previously uninvestigated LDs in 3T3-L1 adipocytes. We uncovered distinct regulation of cAMP microdomains by using PDE3 and PDE4 inhibitors alongside PDE3B and PDE4D overexpression. Moreover, we investigated how distinct cAMP microdomains are regulated by FGF1 or insulin.

2 | METHODS

2.1 | Construction of FRET-based cAMP biosensors

The plasmids encoding the cytoplasmic and plasma membranetargeted fluorescent cAMP biosensors were kindly provided by Prof. Viacheslav Nikolaev, UKE Hamburg (Nikolaev et al., 2004). Membrane anchoring was achieved by an additional N-terminal myristoylation signal (MGCINS) in comparison to the untargeted sensor. The sensors consist of an EYFP-EPAC1-CFP construct in a pcDNA3 (Invitrogen) backbone. For the construction of the lipid-droplet-associated biosensor, the cytoplasmic biosensor was linearized with HindIII-HF (R3104. NEB) immediately upstream of the EYFP start codon. Perilipin-1 (NM_001113471.1) was amplified with Q5 polymerase (M0492, NEB, Ipswich, USA) from murine cDNA with primers forward: AAGCT-TATGTCAATGAACAAGGGCCCAAC reverse: AAGCTTCTCGCAGAA-GAAATCCACCAAGGGCATGCTCTTCTTGCGCAGCTG incorporating a flexible C-terminal linker as recommended by V. Nikolaev and HindIII-sites on both ends of the product. The PCR amplicon was also digested with HindIII and vector and insert were used in a 1:6 ratio for cyclization by Quick Ligase (M2200, NEB).

After transformation in 5-alpha competent cells (C2987, NEB), plasmids were isolated and incorporation of the insert in the right orientation was analysed by restriction digest with EcoRI (R0101, NEB) and validated by sequencing. Endotoxin-free plasmids for nucleoporation into 3T3-L1 cells were purified from large-scale cultures with the NucleoBond Xtra Maxi EF kit (740426, Macherey-Nagel, Düren, Germany).

2.2 | Cell culture and in vitro differentiation of 3T3-L1 adipocytes

All experiments were performed with in vitro differentiated 3T3-L1 murine adipocytes (RRID:CVCL_0123). Cells were grown in 100-mm cell culture dishes in a cell culture incubator in a humid atmosphere containing 5% CO₂ and 95% air at 37°C. The 3T3-L1 preadipocytes were differentiated to mature adipocytes as described elsewhere (Sancar et al., 2022). For staining of LDs and plasma membrane adipocytes are treated with 1-µM BODIPY™ 558/568 C12 (D3835, Invitrogen, Carlsbad, USA) for 30 min or 10-µg·ml⁻¹ CF-350 GWA (#29021, Biotium, Fremont, USA) for 10 min, respectively, washed with PBS and visualized with ApoTome.2 microscope (Zeiss, Oberkochen, Germany).

2.3 | Viral PDE overexpression

The 3T3-L1 adipocytes were differentiated in 12 well plates. On the Day 7 of differentiation, medium was changed to growth medium (high glucose, L-glutamine and pyruvate-supplemented DMEM (11995065, Gibco, Waltham, USA with 10% FBS (A5256701, Gibco), 10-mM HEPES [15630056, Gibco] and antibiotic-antimycotic

[15240062, Gibco]) with 5-μg·ml⁻¹ insulin (I6634, Sigma-Aldrich, St. Louis, USA) and 10⁶ genomic copies of virus per cell were added according to previously published methods (Sancar et al., 2022). The adipose-specific adeno-associated viruses (adAAVs) expressing either mouse PDE3B (NM_011055.2) or PDE4D (NM_001402885.1) were kept for 2 days on the cells before nucleoporation with the cAMP biosensors. adAAVs were produced at Viral Core Facility at Charite, Universitätsmedizin Berlin (vcf.charite.de).

2.4 | Nucleoporation of cAMP biosensors into 3T3L1 adipocytes

Cells on day 10 of differentiation were washed with 1-mM EDTA (15,575,020, Invitrogen) in PBS (10010023, Gibco) and detached with Trypsin (25200056, Gibco). Cells were gently washed off the culture vessel with nucleoporation-medium consisting of growth medium without antibiotics-antimycotics but supplemented with 1-μM rosiglitazone (71740, Cayman, Ann Arbor, USA) and 5-µg·ml⁻¹ insulin. The cell suspension was filtered through a 100 µm cell strainer. After counting, cells were pelleted and resuspended to a density of 16.5×10^6 cells per ml of supplemented SE cell line 4D-Nucleofector solution (V4XC-1032, Lonza, Basel, Switzerland). In nucleoporation strips, 20 µl of this suspension was mixed with 1 µg endotoxin-free Plasmid and run with programme CA-133. Following a 5-min recovery phase at room temperature, cells were diluted in nucleoporationmedium and seeded onto collagen I (354236, Corning, Corning, USA)coated eight-well chamber slides (94.6140.802, Sarstedt, Nümbrecht, Germany) in a density of 220,000 cells per well. After 24 h the cells were washed with PBS and kept until the next day in growth medium.

2.5 | Fluorescence live-cell imaging/FRET-based cAMP measurements

On the day of the measurement, the cells were again washed with PBS and fasted for 2–3 h in growth medium with FBS replaced by 0.5% fatty acid-free bovine serum albumin (BSA) (A8806, Sigma-Aldrich). Shortly before starting the FRET measurements, cells were washed twice and covered with Krebs-Ringer Bicarbonate HEPES (KRBH) buffer consisting of 120-mM NaCl, 4-mM KH $_2$ PO $_4$, 1-mM MgSO $_4$, 0.75-mM CaCl $_2$, 10-mM NaHCO $_3$, 30-mM HEPES, 5-mM glucose and 0.1% BSA. Inhibitors and hormones were added 30 and 15 min, respectively, before the start of the measurements at the following concentrations: 15- μ M cilostamide (iPDE3, 231085, Sigma-Aldrich), 5- μ M roflumilast (iPDE4, SML1099, Sigma-Aldrich), 100-nM insulin and 100-ng·ml $^{-1}$ FGF1 (97056, Biomol, Hamburg, Germany).

Cells were analysed using a Zeiss AXIO Observer Z1 (Carl Zeiss) with an EC Plan-Neofluar 20X/0.50 objective (Carl Zeiss). Illumination was performed by a LEDHub high-power LED light engine (OMI-CRON Laserage, Rodgau-Dudenhofen, Germany) with a 455-nm LED followed by a 427 \pm 5-nm emission filter (AHF Analysentechnik, Tübingen, Germany). Optical filters included a 459/526/596 dichroic

on [15/10/2025]. See the Terms

Wiley Online Library for rules of use; OA

mirror and a 475/543/702 emission filter (AHF Analysentechnik). The Optosplit II emission image splitter (Cairn Research) was equipped with a T505lpxr long-pass filter (AHF Analysentechnik) to acquire images simultaneously at 475 (CFP) and 540 nm (FRET) with a pco. panda 4.2 bi-sCMOS camera (Excelitas PCO, Kelheim, Germany). To acquire images of cells in multiple regions over time in a measurement, a BioPrecision2 automatic XY-Table (Ludl Electronic, Hawthorne, USA) was used. During the measurements, the cells were kept at 37°C with the ibidi Temperature Controller (Ibidi, Gräfelfing, Germany).

Baseline was recorded for 12-15 min. Then, the cells were stimulated with cAMP-increasing or mimicking agents like isoproterenol (16504, Sigma-Aldrich), forskolin (25 μM, F6886, Sigma-Aldrich), IBMX (100 μM, I7018, Sigma-Aldrich), or the cAMP analogue 8-Bromo-2'-O-methyl-cAMP-acetoxymethyl ester (1–300 μM, B 028, Biolog) were added either alone or successively by manually pipetting the drugs to the respective wells at the indicated timepoints. In experiments testing the modulability of the biosensors in comparison to IBMX and Forskolin, isoproterenol was used in a final concentration of 1 µM, while for all other experiments, 100 nM was used. Image acquisition and control of the microscope was performed using VisiView software (Visitron Systems: RRID:SCR 022546). The raw data of fluorescence over time was exported to Microsoft Excel (Microsoft; RRID:SCR_016137), the background was subtracted, and the FRET ratio (CFP/FRET) was calculated. Additionally, the FRET ratio was then bleaching corrected using the one-phase decay curve fit from GraphPad Prism 10.4.1 software for Windows (GraphPad Software; RRID:SCR 002798).

2.6 RNA extraction, cDNA synthesis and qPCR

Cells were lysed with QIAzol™ Lysis Reagent (79306, Qiagen, Hilden, Germany), and after a chloroform extraction, RNA was isolated with the NucleoSpin® RNA kit (740933, Macherey-Nagel), including a DNase digest, according to the manufacturer's instructions. RNA concentration and purity were assessed via spectrophotometry. Reverse transcription of up to 500 ng RNA was performed with the Transcriptor First Strand cDNA Synthesis Kit (04897030001, Roche, Basel, Germany), using the following run conditions: 25°C for 10 min, 55°C for 30 min and 85°C for 5 min. qPCRs were run as technical triplicates on a LightCycler® 480 Instrument II (Roche) using the PowerTrack™ SYBR Green Master Mix (A46109, Applied Biosystems). The thermal cycling conditions included an initial denaturation at 95°C for 2 min, followed by 45 cycles of 15 s at 95°C, 30 s at 60°C and a 1-s acquisition at 72°C. Melting curves were collected to analyse unspecific amplification, and notemplate controls were included for each gene. Relative gene expression was calculated in LightCycler Software (Roche; RRID:SCR_012155) using the $2^{-\Delta\Delta}$ Ct method, with m36b4 as the reference gene and DMSOtreated cells as the control. The genes and primers used were as follows:

 m36b4 (AGATTCGGGATATGCTGTTGGC/TCGGGTCCTAGAC-CAGTGTTC),

- Pde3b (AAAGCGCAGCCGGTTACTAT/CACCACTGCTTCAAGTCC-CAG) and
- Pde4d (TTTTGCCAGTGCAATACATGATG/CAGAGCGAGTTCC-GAGTTTGT).

2.7 | Lipolysis

The 3T3-L1 adipocytes were pretreated with drugs as in cAMP measurements. Lipolysis was then stimulated by 100-nM isoproterenol. After 4 h of incubation, supernatants were collected, and NEFA concentrations were quantified using the NEFA-HR(2) assay kit (994-91801 and 990-91901 Wako, Neuss, Germany). For the overexpression of PDEs, adipocytes were transduced with adAAVs 4 days before the experiments. Values were normalized to sample volume and total protein content determined by bicinchoninic acid protein assay (23227, Pierce).

2.8 | Statistical analysis

Statistical and data analyses were conducted in accordance with the British Journal of Pharmacology's guidelines (Curtis et al., 2025) on experimental design and analysis. Our studies were designed to generate groups of equal size using similar treatment conditions within the same experiment. Randomization was achieved by assigning treatments to different wells on multiwell slides in a random order each measuring day. Blinding was not performed during analysis, as the focus of the study was on the technical validation of the biosensors and treatments, and the risk of observer bias was considered minimal given the objective nature of the measurements. Sample size was determined using power analysis (G*Power, Faul et al., 2007; RRID: SCR_013726), assuming an effect size of 30%, variance of 15%, $\alpha = 0.05$ and 80% power. This yielded a required sample size of n = 4 per group. Basic calculations, determination of outliers, calculations of area under the curve (AUC) and Levene's test were performed with R Statistical Software (v4.4.2; Team, 2024; RRID:SCR 001905). Outliers were identified and excluded with the interquartile range (IQR) method implemented in the rstatix package (Kassambara, 2023; RRID: SCR 021240). The number of excluded datapoints for each reporter or treatment is provided in Table S2. The caTools package (Tuszynski, 2024; RRID:SCR_023566) was used for AUC calculations, and homoscedasticity was tested with Levene's Test from the car package (Fox & Weisberg, 2019; RRID:SCR_022137). GraphPad Prism was used for additional statistical analyses and data visualization. For pairwise comparisons, data normality was first assessed by Shapiro-Wilk test. Normally distributed data were analysed using a paired t-test, while non-normally distributed data were analysed with Wilcoxon signed-rank test. For repeated measurement comparisons, a Friedman test was conducted, followed by Dunn's post hoc test to determine pairwise differences. To compare data between multiple groups, normality was assessed with the Shapiro-Wilk test. If the data were normally distributed, homogeneity of variances was verified with

Levene's test. If both assumptions were met, a one-way ANOVA was performed, followed by Tukey's post-hoc test only if the F-value was significant (P < 0.05). In cases of normally distributed, heteroscedastic data, Welch-ANOVA was employed and followed either by Dunnett's T3 (for small sample sizes) or Games-Howell (for >50 samples per group) post hoc test, again only if the F value was significant.

Post-hoc tests were run only if F achieved P<0.05 and there was no significant variance inhomogeneity. If normality was violated, a Kruskal–Wallis test was used with Dunn's post hoc test only if the Kruskal–Wallis result was significant. For all analysis, statistical significance was set at a *P* value of less than 0.05 and this threshold was not varied in the presentation of results. Statistical tests were not applied to data from Groups with fewer than five independent measurement days (n < 5), and the findings should be interpreted with caution and require validation in future studies with larger sample sizes. Due to the limited sample size, these results are considered preliminary. The number of individual cells, traces, datapoints and independent experiments for each figure and supporting figure is provided in Table S1.

Y axis labels for FRET data display either Absolute Ratio CFP/FRET or Normalized Ratio CFP/FRET, and for lipolysis data, we report μmol NEFA/mg protein. For figures showing normalized FRET ratios (on the y axis), the FRET response at each time point was divided by the mean baseline response (average of the first 5 min) of the same trace. This normalization allows for the comparison of fold changes relative to the cell's individual baseline and ensures that the data are expressed as fold change relative to the baseline for each individual trace, in accordance with the corresponding Y axis labelling in the figures. This approach minimizes unwanted sources of variation, such as differences in initial baseline activity across cells, ensuring that observed effects are reflective of changes induced by experimental treatments rather than inherent variability.

2.9 Nomenclature of targets and ligands

Key protein targets and ligands in this article are hyperlinked to corresponding entries in https://guidetopharmacology.org, and are permanently archived in the Concise Guide to PHARMACOLOGY 2023/24 (Alexander, Christopoulos et al., 2023) and (Alexander, Fabbro et al., 2023).

3 | RESULTS

3.1 | Establishment of pm-cAMP, cyt-cAMP and LD-cAMP biosensors in adipocytes

We used EPAC-based cAMP biosensors that are targeted to cytoplasm (cyt-cAMP) (Nikolaev et al., 2004) or the plasma membrane with a lipid anchor (pm-cAMP) (Zacharias et al., 2002) and generated an LD-associated cAMP biosensor (LD-cAMP) (Figure 1a). We confirmed the uniform distribution of cyt-cAMP and association with the plasma membrane for pm-cAMP in adipocytes, as previously observed in

other cell types (Kannabiran et al., 2020; Terrin et al., 2006) (Figures 1a and S1a). Our newly generated LD-cAMP biosensor, as deduced from fusion to the LD-associated protein perilipin-1, is localized in the vicinity of the LDs (Figure 1a, right panel). We tested the sensitivity of the biosensors using the cell-permeable cAMP analogue 8-Br-2'-O-Me-cAMP-AM in adipocytes. All three reporters responded to the cAMP analogue treatment, albeit with different FRET signal intensity (Figures 1b and S1b). The pm-cAMP biosensor responded with less fluorometric changes compared to cyt-cAMP and LD-cAMP in all 8-Br-2'-O-Me-cAMP-AM concentrations tested (Figures 1b and S1b,c). The responses of the cyt-cAMP and LD-cAMP were comparable, especially in the upper end of the dose-response curve. In adipocytes, one of the main compounds used to study lipolysis in vitro is isoproterenol (ISO), which can activate all β -adrenoceptors, thereby activating robust lipolytic action through cAMP/PKA (Galitzky et al., 1995; Van Liefde et al., 1992). We tested the response of our biosensors to ISO followed by forskolin/IBMX treatment to trigger a maximum endogenous cAMP response (Figure 1c). The plasma membrane cAMP biosensor showed a lower fold response to ISO and forskolin/IBMX treatment compared to cyt-cAMP, potentially indicating a generally lower efficacy of pm-cAMP (Figure S1d). Single fluorescence intensities of Yellow Fluorescent Protein (YFP) and Cvan Fluorescent Protein (CFP) confirmed the expected behaviour from the FRET response (Figure S1e). Interestingly, the ISO-induced FRET signal was much higher for the LD-cAMP compared to the cyt-cAMP biosensor despite a similar response to the EPAC-specific cAMP analogue (Figures 1d and S1d). The cyt-cAMP exhibited a faster adaptation to ISO treatment, as indicated by a transient response, whereas in LDcAMP, the ISO-induced response was more sustained. (Figure S1f). Together, our data indicate the presence of distinct cAMP pools near LDs that are regulated differently from those in the cytoplasm.

3.2 | Inhibiting PDE4 or PDE3 activity reveals distinct cAMP pools regulated by each enzyme

PDE3 and PDE4 activity comprises most of the PDE activity in adipocytes (Choi et al., 2006). However, their contribution to subcellular cAMP microdomains is only investigated using cytoplasmic cAMP biosensors designed to monitor the generation of cAMP at the receptor level in adipocytes (De Jong et al., 2023). To assess the contribution of PDE3 and PDE4 activity to the cAMP regulation in different subcellular compartments, we tested the effect of the specific inhibitors cilostamide (iPDE3) or roflumilast (iPDE4) on ISO-induced cAMP dynamics. To distinguish effects on basal cAMP levels from responses provoked by β -adrenoceptor stimulation, we analysed both absolute FRET ratios and values normalized to baseline. This is important to identify compounds shifting basal levels that could consequently mask or exaggerate effects throughout the entire measurement, while upon normalization ISO-induced fold changes are revealed more clearly. Hence, absolute traces are presented to determine the effect of treatment on basal cAMP dynamics before ISO stimulation. Normalized traces are used to identify fold-response to ISO stimulation when the

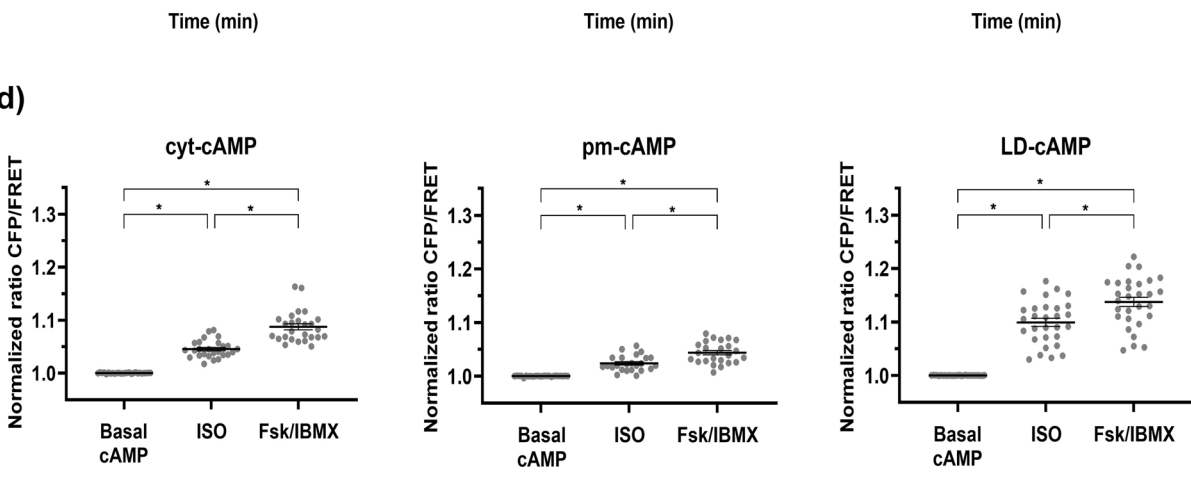


FIGURE 1 Legend on next page.

FIGURE 1 Establishment of cyt-cAMP, pm-cAMP and LD-cAMP biosensors in adipocytes. (a) Design of cAMP biosensors. A fluorescent protein FRET pair (Yellow Fluorescent Protein [YFP] in yellow and Cyan Fluorescent Protein [CFP] in cyan) is connected by Epac1, a cAMP-sensing protein. A lipid anchor (Pal·Myr $^{-1}$) or a lipid droplet binding protein (PLIN1) allows targeting of the plasma membrane and lipid droplets (LDs), respectively. The reporters' localizations were observed by fluorescent imaging with a GFP filter set, and lipid droplets (seen as red) were stained with BODIPY $^{\text{TM}}$ 558/568 C_{12} (scale bar: 20 µm). (b) Normalized traces of cAMP-reporters: arrows indicate the times at which different doses of the cell-permeable Epac1-activator 8-Br-2'-O-Me-cAMP-AM were added. For all traces, the mean \pm SEM is shown. (c) Normalized traces showing the addition of 1-µM isoproterenol (ISO) and a combination of 25-µM Forskolin (Fsk) and 100-µM 3-isobutyl-1-methylxanthine (IBMX) at the indicated time-points. (d) Mean normalized ratios of a 3-min timeframe at baseline or after ISO addition as well as the maximum response after ISO addition from traces depicted in (c) of cyt-cAMP, pm-cAMP and LD-cAMP. Since n, the number of independent values, was n=3 for these studies, statistical analysis was not carried out and results should be regarded as preliminary.

baseline was normalized to one. Inhibition of the PDE3 or PDE4 activity did not change the basal cyt-cAMP levels significantly (Figure 2a,b). Absolute ISO response and acute ISO response (max response within 5 min of ISO addition) were highest when PDE4 activity was inhibited (Figures 2c and S2a). Normalized ISO and normalized acute ISO response were also highest when PDE4 activity was inhibited (Figures 2d,e and S2b). Upon PDE3 inhibition, we observed a higher acute ISO response when the data were normalized to baseline (Figure S2b). Of note, the inhibition of PDE3 or PDE4 activity changed the shape of the ISO response of cyt-cAMP, showing an earlier increase compared to the control condition (Figure 2d). The inhibition of the PDE3 or PDE4 activity did not significantly change the basal pm-cAMP and the absolute ISO response (Figures 2f-h and S2c). However, normalized ISO response was higher when PDE4 activity was inhibited without changing the acute ISO response significantly (Figures 2i,i and S2d). Inhibition of PDE3 or PDE4 activity did not change absolute LD-cAMP ISO response although basal FRET cAMP levels were slightly elevated when PDE4 activity was inhibited (Figures 2k-m and S2e). Normalized ISO response seems to be lower upon PDE3 or PDE4 inhibition, potentially due to slightly enhanced basal levels in LD-cAMP levels (Figures 2n,o and S2f). Overall, PDE3 inhibition had a minor effect on cAMP fold response to ISO stimulation with some increase in the normalized acute ISO response on cytcAMP pool. On the other hand, inhibition of PDE4 activity enhanced either basal or ISO response in all three microdomains tested.

3.3 | PDE4D overexpression but not PDE3B overexpression impaired ISO-induced cAMP responses in all three subcellular domains

While overexpression of PDE3B or PDE4D blunts ISO-induced general cAMP levels and PKA activity, it is not known which subcellular cAMP pools are regulated by PDE3B or PDE4D (Omar et al., 2009; Sancar et al., 2022). We employed our subcellular-targeted sensors to investigate how PDE overexpression specifically impacts cAMP levels in distinct cellular compartments, both under basal conditions and following ISO stimulation. Upon PDE3B or PDE4D overexpression, basal cAMP levels were lower for cyt-cAMP (Figure 3a,b) and overexpression of both PDEs decreased the absolute (Figures 3c and S3a) and normalized (Figures 3d,e and S3b) ISO response. PDE3B overexpression shifted the FRET intensity traces, probably due to its strong suppression of the

basal cAMP level in the cytoplasm (see Figure 3a,b). PDE4D expression had a less prominent but still significant effect on basal cyt-cAMP, while it suppressed the cyt-cAMP response to ISO in a solid manner compared to PDE3B overexpression (see Figure 3d,e). Concerning pmcAMP, AAV-mediated PDE3B or PDE4D overexpression did not alter basal cAMP or the absolute ISO response significantly (Figures 3f-h and S3c). PDE3B or PDE4D overexpression decreased the foldresponse to ISO and acute ISO response when normalized to basal while PDE4D overexpression showed a more robust difference (Figures 3i,j and S3d). For the LD-cAMP, in cells overexpressing PDE4D, basal cAMP levels were lower, whereas cells overexpressing PBE3B showed no change in basal cAMP (Figure 3k,I). Furthermore, we observed a decreased absolute and normalized ISO response upon PDE4D overexpression (Figures 3m-o and S3Ee,f). PDE3B overexpression decreased only the normalized acute ISO response (Figure S3f). Overexpression of Pde3b and Pde4d was confirmed by gene expression analysis (Figure S3g). Consistent with the PDE inhibitor experiments, which revealed that PDE4 inhibition has a stronger effect compared to PDE3 inhibition, overexpression of PDE4D resulted in a more robust response in preventing ISO-induced cAMP changes compared to PDE3B overexpression in all three microdomains tested.

3.4 | Antilipolytic hormones FGF-1 and insulin target distinct cAMP pools

Although both insulin and FGF-1 can suppress lipolysis in adipocytes, it is not known whether they regulate distinct cAMP pools. Hence, we tested whether there is a distinct effect of FGF-1 or insulin on ISOinduced cAMP responses using our subcellular targeted cAMP biosensors. Insulin and FGF-1 treatment decreased both basal and ISOinduced absolute cyt-cAMP levels, with insulin showing a stronger effect compared to FGF-1 (Figures 4a-c and S4a). Normalized ISO response was slightly lower upon insulin or FGF-1 treatment without changing the normalized acute ISO response (Figures 4d,e and S4b). Basal pm-cAMP FRET signals trended to lower values upon FGF-1 treatment, but this was not statistically significant (Figure 4f,g). Insulin did not exhibit a significant effect on the ISO-induced pm-cAMP response (Figures 4h-j and S4c,d), whereas FGF1 decreased the normalized acute ISO response (Figure S4d). For the LD-cAMP biosensor, insulin decreased the basal cAMP levels, whereas FGF-1 treatment was similar to vehicle (Figure 4k,I). Neither FGF-1 nor insulin changed

14765381, 0, Downloaded from https://bpspubs.onlinelibrary.wiley.com/doi/10.1111/bph.70216 by Helmholtz Zentrum Muenchen Deutsches Forschungszentrum, Wiley Online Library on [15/10/2025]. See the Terms

onditions) on Wiley Online Library for rules of use; OA articles are governed by the applicable Creative Commons License

FIGURE 2 Inhibiting PDE4 or PDE3 activity reveals distinct cAMP pools regulated by each enzyme. (a, f, k) Absolute traces of reporter-expressing cells pre-treated with vehicle (DMSO, grey), PDE3 inhibitor (purple, 15- μ M cilostamide = iPDE3) or PDE4 inhibitor (orange, 5- μ M roflumilast = iPDE4). Addition of isoproterenol (ISO) is marked by an arrow. (b, g, I) Basal cAMP levels after incubation with PDE-inhibitor as averages from minutes 0–5. (c, h, m) The average of the plateau post ISO-treatment ranging from minutes 10–15, was compared between different treatments for each reporter. (d, i, n) Normalization was performed for every individual trace from (a), (f) and (k) to its own basal cAMP level. (e, j, o) The ISO response as depicted in (c), (h) and (m) but for normalized traces. Panels (a)–(e) for cytosolic, (f)–(j) for plasma membrane and (k)–(o) for lipid-droplet associated cAMP biosensor. All traces are shown as mean \pm SEM. Since n, the number of independent values, was n=4 for PDE3 studies, statistical analysis was not carried out and those results should be regarded as preliminary. The statistical significance is depicted as ns: not significant and * P < 0.05.

the absolute ISO responses of LD-cAMP (Figures 4m and S4e), suggesting that the antilipolytic actions of both hormones are not transduced to this compartment of the adipocyte. Normalized response to ISO was slightly higher upon FGF-1 or insulin pre-treatment, probably due to slightly lower basal levels (Figures 4n,o and S4f). Together, our data suggested that while FGF-1 potentially targets the pm-cAMP pool, insulin was more robust at decreasing cyt-cAMP levels. Interestingly, the LD-cAMP ISO responses remained largely unaffected by either antilipolytic hormone.

3.5 | Antilipolytic effects of FGF-1, insulin and PDEs correlate with cAMP modulation

In order to correlate the effects that we described for PDEs and antilipolytic hormones on the distinct cAMP pools to the extent of lipolysis regulation, we measured lipolysis in adipocytes under the same conditions as in our cAMP-FRET measurements (Figures 1–4). Overexpression of PDE4D had a more robust effect in suppressing lipolysis compared to the overexpression of PDE3B (Figure 5a). This is in agreement with a more potent downregulation of cAMP levels by PDE4D overexpression in all three pools tested. In accordance, inhibition of PDE4 activity resulted in higher lipolysis compared to PDE3 inhibition (Figure 5b). While it has been previously published (Sancar et al., 2022), we tested antilipolytic potential of FGF-1 or insulin treatment side-by-side and observed that insulin is more potent in suppression of lipolysis compared to FGF-1 (Figure 5b).

Some conclusions regarding the effects of treatments with cAMP-mimicking and cAMP-increasing drugs (Figure 1), iPDEs (Figure 2), PDE overexpression (Figure 3) and lipolysis (Figure 5) are based on data from fewer than five independent experiments (n < 5) hence could be considered as preliminary.

4 | DISCUSSION

In this study, we have investigated subcellular cAMP levels in adipocytes and identified a previously unrecognized cAMP compartment surrounding LDs that is distinct from cytoplasmic cAMP. While a comparison of cytoplasmic cAMP vs plasma membrane cAMP pools was employed in other cell types, to our knowledge our study is the first to investigate their comparison in adipocytes. We used a pm-cAMP biosensor targeted to lipid rafts where the majority of the receptor

signalling is concentrated via lipid-protein and protein-protein interactions (Agarwal et al., 2014). To measure cAMP pools surrounding the LDs, we used perilipin-1 which is exclusively localized at LDs, as previously described (Hsieh et al., 2012; Sancar et al., 2022). Overall, we observed strong and comparable responses in cyt-cAMP and LDcAMP upon ISO stimuli and a weaker response in the pm-cAMP biosensor. When a cAMP analogue was employed, the pm-cAMP FRETresponse was weaker than that of the other biosensors indicating the possible max fold response ratio is lower in general with this cAMP reporter when it is directed to lipid rafts and/or modified with myristoylation/palmitoylation. The sensitivities of the cytosolic cAMP and LD-associated cAMP biosensors were comparable, particularly at higher concentrations of the cAMP analogue. However, at lower cAMP levels, the cytosolic biosensor exhibited greater sensitivity than the LD-targeted sensor. Therefore, while the effects of different treatments can be reliably compared within each individual biosensor, the absolute magnitude of responses should not be directly compared across the biosensors herein. The adaptation following ISO stimulation differed between cyt-cAMP and LD-cAMP, with cyt-cAMP exhibiting a faster peak decline and adaptation, whereas the ISO response in LD-cAMP was more stable. One explanation could be a higher PDE activity in the cytosol compared to PDE activity surrounding the LDs. This is supported by the fact that inhibiting PDE3 or PDE4 activity had a stronger effect on the cyt-cAMP compared to LD-cAMP. Moreover, overexpression of PDE4D or PDE3B did not abolish the ISO responses in LD-cAMP pools suggesting less PDE localization on the LDs, even under unphysiological expression conditions.

When analysing cAMP responses using our FRET-based reporters, we used both absolute FRET ratios and ratios normalized to baseline to distinguish different types of compound effects. A compound that alters basal cAMP levels can shift the entire response curve upward or downward, without necessarily affecting the fold change induced by isoproterenol (ISO). Therefore, analysing absolute FRET ratios allows us to detect changes in basal activity, while normalization to baseline helps isolate effects on β -adrenoceptor responsiveness (i.e., the fold induction upon ISO stimulation). This dual approach allows us to distinguish between compounds that affect baseline levels versus those that modulate dynamic signalling responses, giving a more comprehensive understanding of compound effects.

Previously, cytoplasmic cAMP levels were measured using EPAC1-camps biosensors in white and brown adipocytes and indicated distinct cAMP pools generated by different β -adrenoceptors (De Jong et al., 2025; Kannabiran et al., 2020). While we used ISO

1476581, 0, Downloaded from https://bpspubs.onlinelibrary.wiley.com/doi/10.1111/bph.70216 by Helmholtz Zentrum Muenchen Deutsches Forschungszentrum, Wiley Online Library on [15/10/2025]. See the Terms

onditions) on Wiley Online Library for rules of use; OA articles are governed by the applicable Creative Commons

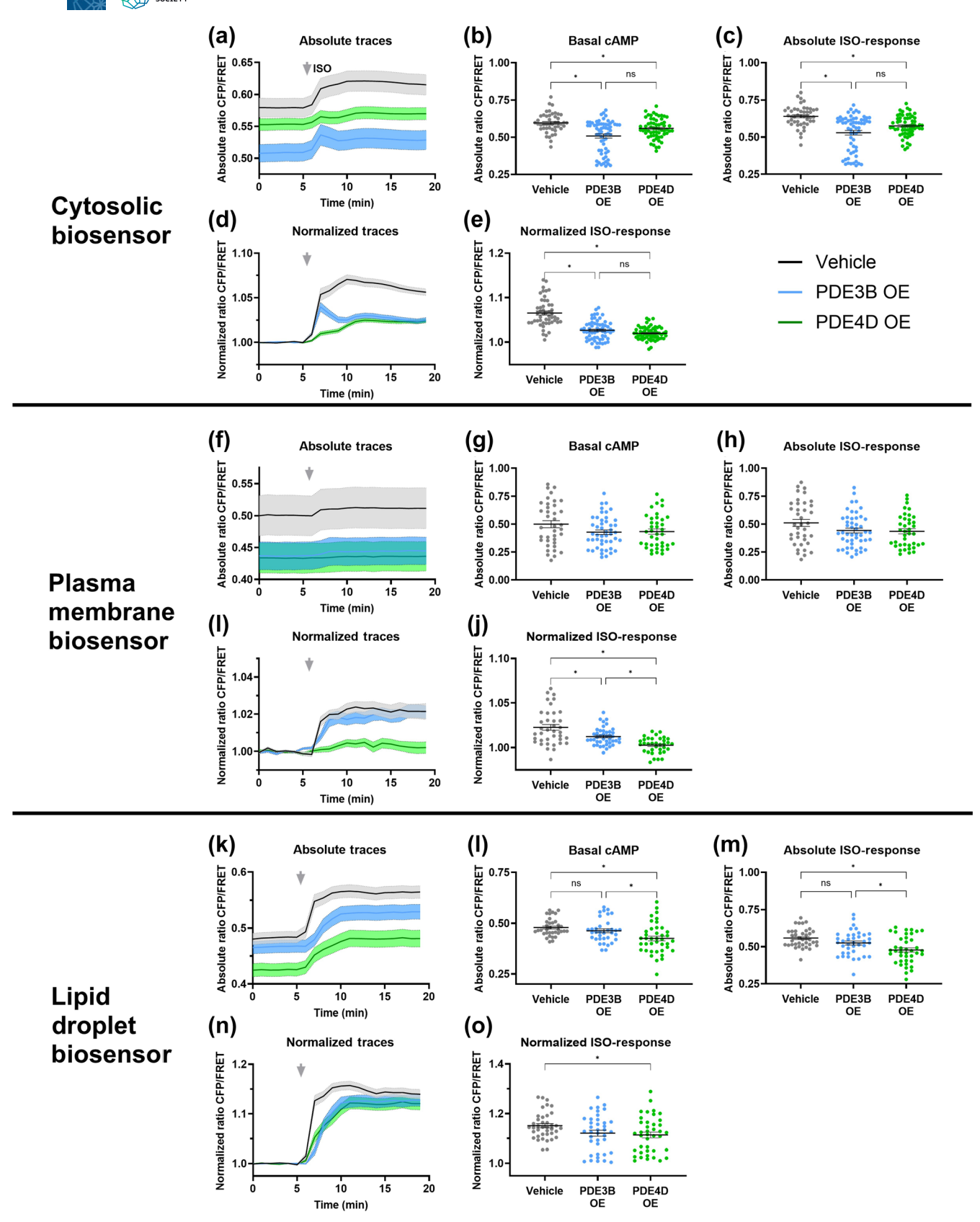


FIGURE 3 Legend on next page.

FIGURE 3 PDE4D overexpression but not PDE3B overexpression impaired ISO-induced cAMP responses in all three subcellular domains. (a, f, k) Absolute cAMP traces of reporter-expressing cells (grey) additionally treated with adAAVs leading to expression of PDE3B (light blue) or PDE4D (green). The addition of isoproterenol (ISO) is marked by an arrow. (b, g, I) Basal cAMP levels measured from 0–5 min at baseline. (c, h, m) Comparison of the post-ISO plateau phase (10–15 min) between treatments for each reporter. (d, i, n) Normalization of individual traces from panels (a), (f) and (k) to their respective basal cAMP levels. (e, j, o) ISO response from panels (c), (h) and (m) but for normalized traces. Panels (a)–(e) for cytosolic, (f)–(j) for plasma-membrane and (k)–(o) for lipid-droplet-associated cAMP biosensor. All traces represent mean ± SEM. Since n, the number of independent values, was between 3–4 for these studies, statistical analysis was not carried out and results should be regarded as preliminary.

which activates $\beta 1/\beta 2$ and partially $\beta 3$ -adrenoceptors to stimulate cAMP production at the concentration we used, we did not differentiate between the generation of the cAMP pools at the receptor but rather focused on how PDEs or antilipolytic hormones such as FGF-1 or insulin affect the cAMP pools in different subcellular localizations. Inhibition of PDE4 activity had an enhanced ISO-induced normalized response in pm-cAMP and cyt-cAMP regions but did not increase ISO response on LD-cAMP. While the effect of PDE4 inhibitors on pmcAMP can be attributed to the involvement of PDE4 in signal generation (see below), the impact on cyt-cAMP is likely due to the cytoplasmic abundance of PDE4s combined with increased cAMP production due to enhanced β-adrenoceptor signalling. The 'resistant nature' of LD-cAMP to PDE4 inhibitors indicates either that the generation of cAMP surrounding LDs is regulated differently than for the rest of the cAMP or that there is exclusion of PDEs from the LD compartments in a normal state. The existence of organelle-LD contact sites was previously suggested in other cell types, but plasma membrane-LD contact sites have not been thoroughly investigated in adipocytes (Dudka et al., 2010; Liao et al., 2022; Robenek et al., 2005). If there are β-adrenoceptor signalling domains in the close vicinity of the LDs with different protein complexes devoid of PDEs, this could explain why inhibition of PDE4 or PDE3 had a minimal effect on LD-cAMP.

In mouse 3T3-L1 adipocytes, PDE4D overexpression was more potent in the suppression of cAMP levels compared to PDE3B overexpression in all three microdomains we investigated. This seems to contradict our current understanding that PDE3B is the main PDE responsible for the antilipolytic actions of insulin. However, our observation may be partly explained by the fact that PDE3B must be activated through phosphorylation in response to external stimuli like insulin, as mere overexpression does not ensure active PDE3B. Thus, it would be of interest to investigate whether FGF-1 or insulin treatment further potentiates PDE4D or PDE3B overexpression as treatment with both results in phosphorylated and activated PDE4D (Sancar et al., 2022). Inhibition of PDE3 or PDE4 activities by specific inhibitors suggested that PDE4 inhibition had stronger effects on cAMP compared to PDE3 inhibition in 3T3-L1 adipocytes. While inhibiting either PDE activity alone increases lipolysis, inhibition of both simultaneously produces an even greater synergistic effect, suggesting compensation and/or cross-talk between the PDEs (Snyder et al., 2005; Wang & Edens, 2007). It was shown that both PDE4D and PDE3B can be activated by PKA (Lim et al., 1999; Palmer et al., 2007). Hence, it is expected that when PDE3B activity is inhibited, enhanced cAMP/PKA activity could activate PDE4D to prevent further cAMP/PKA/lipolysis increase. Another possible explanation is that PDE4D overexpression targets the production of cAMP in

response to ISO treatment. Since PDE4D overexpression strongly blunted pm-cAMP response, it is possible that overexpressed PDE4D localized to the β -adrenoceptors could inhibit the production of cAMP at the source, preventing its distribution to the cytoplasm or LD. In other cellular systems, localization of PDE4D to β-adrenoceptors via recruitment by β -arrestins and decrease of cAMP levels has been shown (Perry et al., 2002; Richter et al., 2008; Shi et al., 2017). Moreover, PDE4s are generally found in soluble form in cytoplasm hence, overexpression of PDE4D can degrade the rest of the cAMP that is generated upon ISO stimulation, while PDE3B is mainly localized in the insoluble fractions such as endoplasmic reticulum (Jin et al., 1998; Shakur et al., 2000). We were able to decrease the LD-cAMP response and basal levels only when we overexpressed PDE4D. This could be due to the strong effect of PDE4D overexpression on generation (pmcAMP) and propagation (cyt-cAMP) of the cAMP. Another possibility is a potential localization of the PDE4D on the LDs upon overexpression which would locally degrade cAMP on the LD. Studies focusing on the localization of PDE3B and PDE4D upon basal and overexpressed levels and the effect of lipolytic (ISO) or antilipolytic stimuli like FGF-1 and insulin on their localization will unravel the molecular mechanisms explaining the effect on subcellular cAMP pools.

Our study highlights the distinct mechanisms by which the antilipolytic hormones FGF-1 and insulin inhibit the cAMP/PKA pathway. While FGF-1 targets strongly the generation of cAMP as determined by a blunted pm-cAMP response, insulin decreases the overall cAMP levels in the cytoplasm with a minor effect on the pm-cAMP. The minimal effect of FGF-1 on cyt-cAMP was unexpected as FGF-1 efficiently blunted the generation of the pm-cAMP response. One possible explanation would be that other β-adrenoceptors that are not localized to lipid rafts could continue to induce cAMP production raising the cAMP pools directly in the cytoplasm. Previous studies have shown that an increase in cytoplasmic cAMP does not necessarily correlate with the extent of lipolysis. Importantly, the spatial compartment in which cAMP is produced, and not the total amount of cAMP generated, plays a crucial role, suggesting the involvement of distinct cAMP pools at the receptor level, as recently proposed (Kannabiran et al., 2020; De Jong et al., 2023). Accordingly, higher cAMP levels that are, for example, induced by forskolin are less lipolytic compared to lower cAMP levels that are produced upon ISO stimulation of β -adrenoceptors (Mowers et al., 2013).

The comparison of antilipolytic activity of PDEs, FGF-1 and insulin with their regulation of subcellular cAMP pools reveals that the greater the suppression of cAMP, the higher the antilipolytic activity. For example, PDE4 inhibition or PDE4D overexpression has a stronger effect on ISO-induced cAMP in all three subcellular localizations tested compared

14765381, 0, Downloaded from https://bpspubs.onlinelibrary.wiley.com/doi/10.1111/bph.70216 by Helmholtz Zentrum Muenchen Deutsches Forschungszentrum, Wiley Online Library on [15/10/2025]. See the Terms

onditions) on Wiley Online Library for rules of use; OA articles are governed by the applicable Creative Commons License

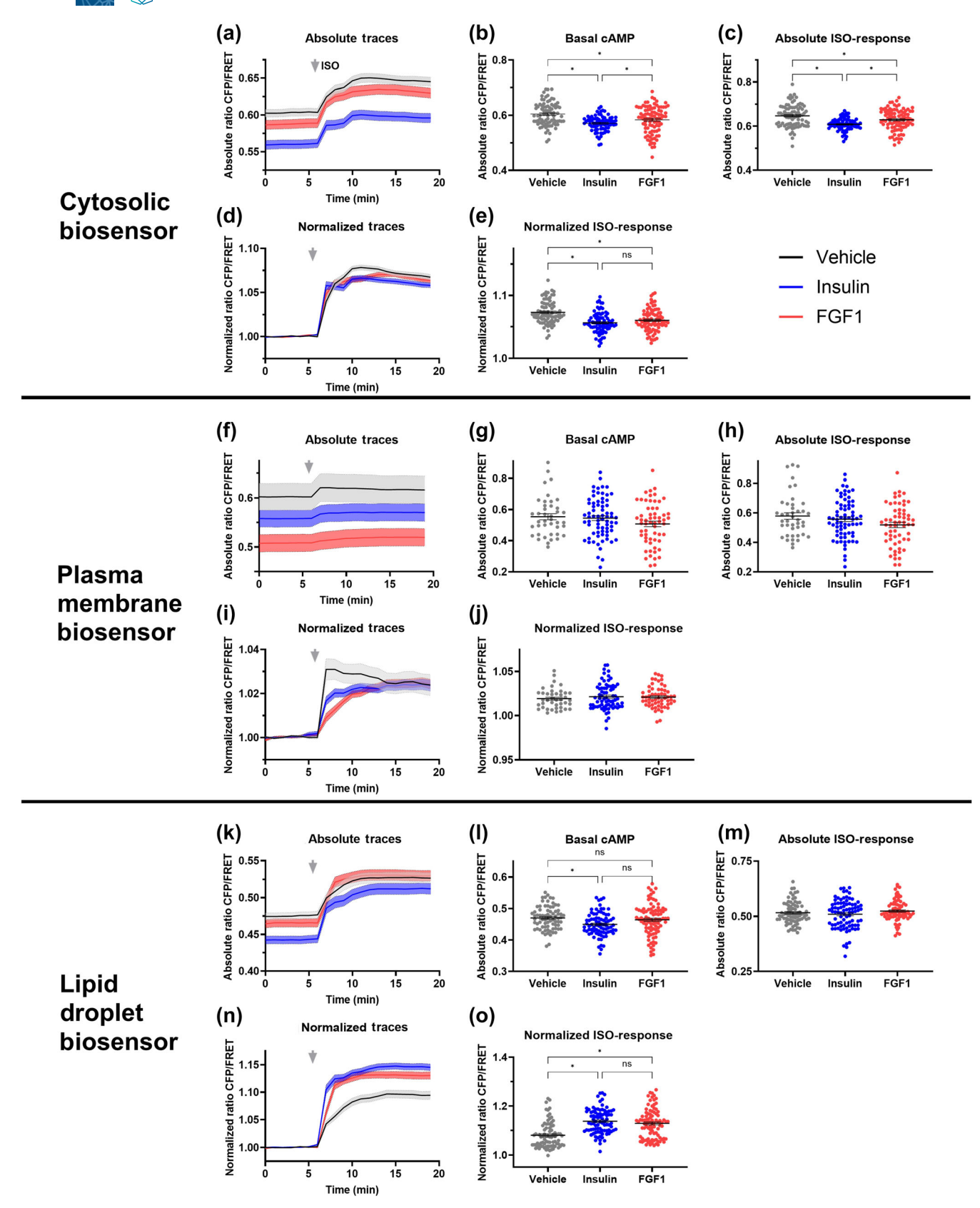


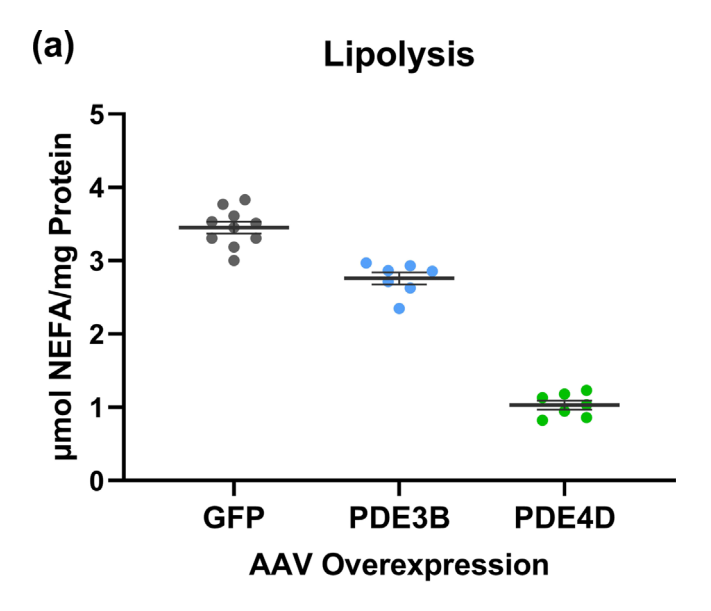
FIGURE 4 Legend on next page.

14765381, 0, Downloaded from https://bpspubs.onlinelibrary.wiley.com/doi/10.1111/bph.70216 by Helmholtz Zentrum

Wiley Online Library on [15/10/2025]. See the Terms

on Wiley Online Library for rules of use; OA articles are governed by the applicable Creative Common

FIGURE 4 Antilipolytic hormones FGF1 and insulin target distinct cAMP pools. (a, f, k) Representative absolute cAMP traces from reporter-expressing cells pre-treated with either vehicle (Krebs-Ringer Bicarbonate HEPES [KRBH], grey), insulin (100 nM, blue) or FGF1 (100 ng·ml $^{-1}$, red). The addition of isoproterenol (ISO) is marked with an arrow. (b, g, l) Basal cAMP levels recorded over the first 5 min of the experiment after hormone or KRBH pre-treatment. (c, h, m) Mean plateau cAMP levels after isoproterenol stimulation (10–15 min), comparing the effects of different antilipolytic treatments across all reporters. (d, i, n) Each individual trace from (a), (f) and (k) was normalized to its own baseline cAMP level. (e, j, o) Normalized ISO response levels, as shown in (c), (h) and (m) but based on normalized traces. Panels (a)–(e) for cytosolic, (f)–(j) for plasma membrane and (k)–(o) for lipid-droplet-associated cAMP biosensor. All traces are expressed as mean \pm SEM, n = 5. Statistical significance is indicated as ns (not significant) and * P < 0.05.



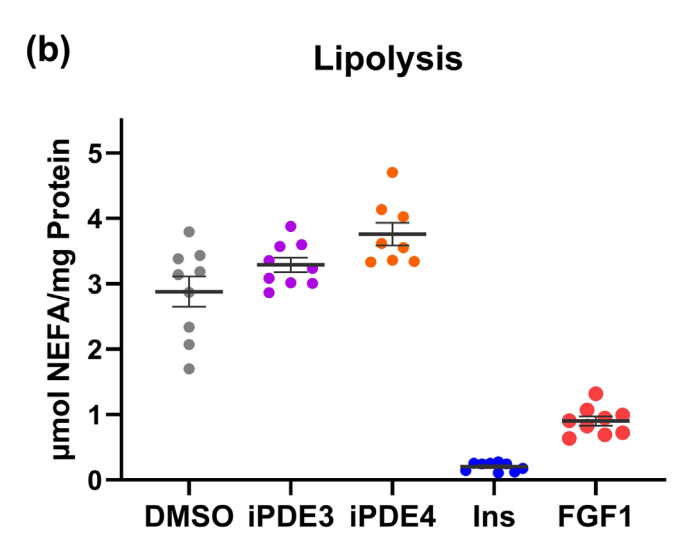


FIGURE 5 Effects of PDE modulation or FGF1/insulin treatment on lipolysis. (a) Quantification of lipolysis in 3T3-L1 adipocytes after overexpression of GFP (as a control), PDE3B or PDE4D using adAAVs. Data are shown as mean ± SEM. Statistical significance is depicted as * P < 0.05. (b) Quantification of lipolysis in 3T3-L1 adipocytes after treatment with vehicle (DMSO, grey), PDE3 inhibitor (purple, 15-μM cilostamide = iPDE3), PDE4 inhibitor (orange, 5-μM roflumilast = iPDE4), insulin (blue, 100 nM) or FGF1 (red, 100 ng·ml $^{-1}$). Data are shown as mean ± SEM. Since n, the number of independent values, was <5 for these studies (n = 3 for (a) and n = 2 for (b)), statistical analysis was not carried out and results should be regarded as preliminary.

to PDE3B, potentially results suggesting a stronger effect of PDE4 on lipolysis. Although cAMP-independent effects of insulin on lipolysis cannot be excluded, (Londos et al., 1985; Strålfors & Honnor, 1989) insulin suppresses lipolysis more strongly than PDE3B overexpression, despite both interventions having strong suppressive effects on cytosolic cAMP levels. Notably, both insulin treatment and PDE4D overexpressioneach showing the strongest suppression of lipolysis—also reduced basal cAMP levels specifically in the LD-associated cAMP pool. Future investigations into the LD proteome and phosphoproteome following insulin stimulation or PDE4D overexpression could help elucidate the molecular changes responsible for modulating lipolysis in adipocytes on the LDs. Recently, the contribution of subcellular cAMP microdomains in regulating lipolysis in human white adipocytes was investigated at the beta-adrenergic receptor level (De Jong et al., 2023). The study reported that insulin resistance disrupts these cAMP microdomains downstream of β-adrenoceptors and results in a change of β-adrenoceptor subtypes in signalling initiation from β1-adrenoceptor to β 3-adrenoceptor for induction of lipolysis. Moreover, instead of PDE3 activity, PDE4 activity is responsible for the cessation of the lipolytic signal in insulin-resistant adipocytes. This is particularly interesting while both in vitro and in vivo models of insulin resistance suggest decreased PDE3B levels in adipocytes (Rahn Landström et al., 2000; Tang et al., 1999). Potentially, PDE4D activity acts as a backup PDE, which compensates for decreased PDE3B levels. In vivo overexpression of PDE4D in adipose tissue was sufficient to normalize impaired glucose metabolism and lipolysis suggesting investigating PDE4 activity in adipose tissue might be more relevant in the context of insulin resistance (Sancar et al., 2022). Among the cAMP pools, the LD-cAMP pool was the least responsive to either PDE inhibitors or FGF-1/insulin treatment for the ISO response in insulin-sensitive adipocytes. It would be of interest to investigate LD-cAMP responses upon insulin resistance to see whether insulin resistance changes the sensitivity of these LDcAMP pools to PDE inhibitors, lipolytic, or antilipolytic signals.

Our study identified previously unrecognized cAMP pools surrounding adipocyte LD, distinct from cytoplasmic cAMP. Using PDE inhibitors revealed that LD-cAMP was largely resistant to PDE3 or PDE4 activity, suggesting unique regulatory mechanisms distinct from cytoplasmic or plasma membrane cAMP pools. PDE4D overexpression suppressed cAMP levels and lipolysis more effectively than PDE3B, potentially due to differences in activation mechanisms or subcellular localization. FGF-1 and insulin exhibited distinct antilipolytic actions, with FGF-1 primarily blunting cAMP generation at the plasma membrane while insulin broadly reduced cytoplasmic cAMP levels. Our data suggest that beyond changes in overall cAMP levels,

Wiley Online Library on [15/10/2025]. See the Terms

Wiley Online Library for rules of use; OA

the spatial location and mechanism of cAMP generation may play important roles in determining the biological functions of the cyclic nucleotide in adipocytes. The findings indicate that cAMP microdomains, particularly pm, and LD-associated pools, may play a crucial role in adipocyte metabolism and could be differentially affected in insulin-resistant states. Using subcellular targeted biosensors for cAMP will play a key role in understanding the molecular changes regulating lipolysis in healthy and insulin-resistant states.

4.1 | Limitations of the study

One limitation of our study was the usage of the 3T3-L1 mouse adipocyte cell line for the establishment of the different biosensors and the effect of PDEs or antilipolytic signals in the previously mentioned microdomains. Relative expression of PDEs might be different in primary mouse or human adipocytes, which limits our findings to the current model we used. For example, inhibition of PDE4 activity had different effects on lipolysis when rat or human adipocytes were used in previously published studies (Nakamura et al., 2004; Snyder et al., 2005). Another limitation is that we used electroporation to express the cAMP biosensors in differentiated adipocytes, which partially affects the viability of the cells and could interfere with their response to various stimuli. It would be of interest to use viral-based expression systems for the cAMP biosensors and compare them with the responses we get via electroporation. While we employed three distinct cAMP biosensors, we acknowledge that their sensitivities are not identical, as also noted by others (Surdo et al., 2017). Therefore, we refrained from directly comparing the magnitude of responses across biosensors. Instead, we focused on how each individual biosensor responded to different treatments using pathologically/physiologically relevant factors such as FGF-1 and insulin. Because groups with fewer than five independent measurement days were included for exploratory analysis, some of the findings should be interpreted as preliminary and require confirmation in larger future studies.

AUTHOR CONTRIBUTIONS

J. Krier: Conceptualization (lead); data curation (equal); formal analysis (lead); methodology (lead); resources (equal); visualization (equal); writing—original draft (equal). D. Spähn: Formal analysis (equal); investigation (Supporting); methodology (Supporting); supervision (Supporting); writing-review and editing (Supporting). D. A. J. Lopez: Methodology (Supporting); validation (Supporting). J. L. Nono: Methodology (Supporting). J. Seigner: Methodology (Supporting). L. Jacob: Methodology (Supporting). S. Ussar: Conceptualization (Supporting); writing-review and editing (Supporting). R. Lukowski: Resources (Supporting); supervision (Supporting); writing-review and editing (Supporting). A. L. Birkenfeld: Funding acquisition (Supporting); funding acquisition (Supporting); resources (Supporting); resources (Supporting); supervision (Supporting); supervision (Supporting). G. Sancar: Conceptualization (lead); funding acquisition (lead); investigation (equal); methodology (equal); project administration (lead); resources (equal); supervision (lead); writing-original draft (lead).

ACKNOWLEDGEMENTS

We would like to thank Viacheslav O. Nikolaev, UKE, Hamburg, for providing cyt-cAMP and pm-cAMP plasmids and feedback on designing the LD-cAMP. We thank the Viral Core Facility (VCF) of the Charite-Universitätsmedizin Berlin for virus production. This work is supported by the German Center for Diabetes Research (DZD), Neuherberg, Germany, and by the German Research Foundation (DFG) via individual grant Bi 1292/12-1 (A. L. B.) and 562635405 (G. S.). A. L. B. is a member of the GRK2816 'Non-canonical G protein signaling pathways: Mechanisms, Functions, Consequences'. Work in the Lukowski laboratory was funded by the German Research Foundation (DFG) via individual grant LU 1490/10-1. R. L. and D. S. are members/associates of the GRK2381: 'cGMP: From Bedside to Bench', DFG Grant Number 335549539. Open Access funding enabled and organized by Projekt DEAL.

CONFLICT OF INTEREST STATEMENT

The authors declare no conflict of interest.

DATA AVAILABILITY STATEMENT

The data that support the findings of this study are available from the corresponding author upon reasonable request. Some data may not be made available because of privacy or ethical restrictions.

DECLARATION OF TRANSPARENCY AND SCIENTIFIC RIGOUR

This Declaration acknowledges that this paper adheres to the principles for transparent reporting and scientific rigour of preclinical research as stated in the *BJP* guidelines for Design and Analysis, and as recommended by funding agencies, publishers, and other organizations engaged with supporting research.

ORCID

Gencer Sancar https://orcid.org/0000-0002-2098-0654

REFERENCES

- Agarwal, S. R., Yang, P. C., Rice, M., Singer, C. A., Nikolaev, V. O., Lohse, M. J., Clancy, C. E., & Harvey, R. D. (2014). Role of membrane microdomains in compartmentation of cAMP signaling. *PLoS ONE*, *9*(4), e95835. https://doi.org/10.1371/journal.pone.0095835
- Ahmad, F., Murata, T., Shimizu, K., Degerman, E., Maurice, D., & Manganiello, V. (2015). Cyclic nucleotide phosphodiesterases: Important signaling modulators and therapeutic targets. *Oral Diseases*, 21(1), e25–e50. https://doi.org/10.1111/odi.12275
- Alexander, S. P. H., Christopoulos, A., Davenport, A. P., Kelly, E., Mathie, A. A., Peters, J. A., Veale, E. L., Armstrong, J. F., Faccenda, E., Harding, S. D., Davies, J. A., Abbracchio, M. P., Abraham, G., Agoulnik, A., Alexander, W., Al-Hosaini, K., Bäck, M., Baker, J. G., Barnes, N. M., ... Ye, R. D. (2023). The Concise Guide to PHARMACOLOGY 2023/24: G protein-coupled receptors. British journal of pharmacology, 180, S23-S144. https://doi.org/10.1111/bph.16177
- Alexander, S. P. H., Fabbro, D., Kelly, E., Mathie, A. A., Peters, J. A., Veale, E. L., Armstrong, J. F., Faccenda, E., Harding, S. D., Davies, J. A., Annett, S., Boison, D., Burns, K. E., Dessauer, C., Gertsch, J., Helsby, N. A., Izzo, A. A., Ostrom, R., Papapetropoulos, A., ... Wong, S. S. (2023). The concise guide to PHARMACOLOGY 2023/24:

- Enzymes. British Journal of Pharmacology, 180(Suppl 2), S289-S373. https://doi.org/10.1111/bph.16181
- Boesch, M., Lindhorst, A., Feio-Azevedo, R., Brescia, P., Silvestri, A., Lannoo, M., Deleus, E., Jaekers, J., Topal, H., Topal, B., Ostyn, T., Wallays, M., Smets, L., Van Melkebeke, L., Härtlova, A., Roskams, T., Bedossa, P., Verbeek, J., Govaere, O., ... van der Merwe, S. (2024). Adipose tissue macrophage dysfunction is associated with a breach of vascular integrity in NASH. *Journal of Hepatology*, 80(3), 397–408. https://doi.org/10.1016/j.jhep.2023.10.039
- Choi, Y. H., Degerman, E., Manganiello, V. C., Park, S., Hockman, S., Zmuda-trzebiatowska, E., Svennelid, F., Haluzik, M., Gavrilova, O., Ahmad, F., & Holst, L. S. (2006). Alterations in regulation of energy homeostasis in cyclic nucleotide phosphodiesterase 3B Null mice find the latest version: Alterations in regulation of energy homeostasis in cyclic nucleotide phosphodiesterase 3B Null mice. *The Journal of Clinical Investigation*, 116(12), 3240–3251. https://doi.org/10.1172/jci24867.3240
- Curtis, M. J., Alexander, S. P. H., Cortese-Krott, M., Kendall, D. A., Martemyanov, K. A., Mauro, C., Panettieri, R. A. Jr., Papapetropoulos, A., Patel, H. H., Santo, E. E., Schulz, R., Stefanska, B., Stephens, G. J., Teixeira, M. M., Vergnolle, N., Wang, X., & Ferdinandy, P. (2025). Guidance on the planning and reporting of experimental design and analysis. *British Journal of Pharmacology*, 182(7), 1413–1415. https://doi.org/10.1111/bph.17441
- De Jong, K. A., Ehret, S., Heeren, J., & Nikolaev, V. O. (2023). Live-cell imaging identifies cAMP microdomains regulating β-adrenoceptor-subtype-specific lipolytic responses in human white adipocytes. *Cell Reports*, 42(5), 112433. https://doi.org/10.1016/j.celrep.2023. 112433
- De Jong, K. A., Siddig, S., Pfeifer, A., & Nikolaev, V. O. (2025). The role of compartmentalized β -AR/cAMP signaling in the regulation of lipolysis in white and brown adipocytes. *The FEBS Journal*, 292(2), 261–271. https://doi.org/10.1111/febs.17157
- DiPilato, L. M., Ahmad, F., Harms, M., Seale, P., Manganiello, V., & Birnbaum, M. J. (2015). The role of PDE3B phosphorylation in the inhibition of lipolysis by insulin. *Molecular and Cellular Biology*, 35(16), 2752–2760. https://doi.org/10.1128/mcb.00422-15
- Dudka, A. A., Sweet, S. M. M., & Heath, J. K. (2010). Signal transducers and activators of transcription-3 binding to the fibroblast growth factor receptor is activated by receptor amplification. *Cancer Research*, 70, 3391–3401. https://doi.org/10.1158/0008-5472.can-09-3033
- Enoksson, S., Degerman, E., Hagström-Toft, E., Large, V., & Arner, P. (1998). Various phosphodiesterase subtypes mediate the in vivo antilipolytic effect of insulin on adipose tissue and skeletal muscle in man. Diabetologia, 41(5), 560–568. https://doi.org/10.1007/s001250050947
- Faul, F., Erdfelder, E., Lang, A.-G., & Buchner, A. (2007). G*power 3: A flexible statistical power analysis program for the social, behavioral, and biomedical sciences. *Behavior Research Methods*, 39(2), 175–191. https://doi.org/10.3758/BF03193146
- Fox, J., & Weisberg, S. (2019). An R companion to applied regression (Third ed.). Sage.
- Galitzky, J., Carpéné, C., Bousquet-Mélou, A., Berlan, M., & Lafontan, M. (1995). Differential activation of beta 1-, beta 2- and beta 3-adrenoceptors by catecholamines in white and brown adipocytes. Fundamental & Clinical Pharmacology, 9(4), 324–331. https://doi.org/10.1111/j.1472-8206.1995.tb00506.x
- Gasser, E., Sancar, G., Downes, M., & Evans, R. M. (2022). Metabolic messengers: Fibroblast growth factor 1. Nature Metabolism, 4(6), 663–671. https://doi.org/10.1038/s42255-022-00580-2
- Gerst, F., Wagner, R., Oquendo, M. B., Siegel-Axel, D., Fritsche, A., Heni, M., Staiger, H., Häring, H. U., & Ullrich, S. (2019). What role do fat cells play in pancreatic tissue? *Molecular Metabolism*, 25, 1–10. https://doi.org/10.1016/j.molmet.2019.05.001

- Hagström-Toft, E., Bolinder, J., Eriksson, S., & Arner, P. (1995). Role of phosphodiesterase III in the antilipolytic effect of insulin in vivo. *Diabetes*, 44(10), 1170–1175. https://doi.org/10.2337/diab.44.10.1170
- Hsieh, K., Lee, Y. K., Londos, C., Raaka, B. M., Dalen, K. T., & Kimmel, A. R. (2012). Perilipin family members preferentially sequester to either triacylglycerol-specific or cholesteryl-ester-specific intracellular lipid storage droplets. *Journal of Cell Science*, 125(Pt 17), 4067–4076. https://doi.org/10.1242/jcs.104943
- Jin, S. L., Bushnik, T., Lan, L., & Conti, M. (1998). Subcellular localization of rolipram-sensitive, cAMP-specific phosphodiesterases. Differential targeting and activation of the splicing variants derived from the PDE4D gene. *Journal of Biological Chemistry*, 273(31), 19672–19678. https:// doi.org/10.1074/jbc.273.31.19672
- Kannabiran, S. A., Gosejacob, D., Niemann, B., Nikolaev, V. O., & Pfeifer, A. (2020). Real-time monitoring of cAMP in brown adipocytes reveals differential compartmentation of β. Molecular Metabolism, 37, 100986. https://doi.org/10.1016/j.molmet.2020.100986
- Kassambara, A. (2023). rstatix: Pipe-Friendly Framework for Basic Statistical Tests.
- Liao, P. C., Yang, E. J., Borgman, T., Boldogh, I. R., Sing, C. N., Swayne, T. C., & Pon, L. A. (2022). Touch and go: Membrane contact sites between lipid droplets and other organelles. Frontiers in Cell and Developmental Biology, 10, 852021. https://doi.org/10.3389/fcell. 2022.852021
- Lim, J., Pahlke, G., & Conti, M. (1999). Activation of the cAMP-specific phosphodiesterase PDE4D3 by phosphorylation. Identification and function of an inhibitory domain. *Journal of Biological Chemistry*, 274(28), 19677–19685. https://doi.org/10.1074/jbc.274.28.19677
- Londos, C., Honnor, R. C., & Dhillon, G. S. (1985). CAMP-dependent protein kinase and lipolysis in rat adipocytes. III. Multiple modes of insulin regulation of lipolysis and regulation of insulin responses by adenylate cyclase regulators. *Journal of Biological Chemistry*, 260(28), 15139–15145. https://doi.org/10.1016/S0021-9258(18)95713-3
- Mowers, J., Uhm, M., Reilly, S. M., Simon, J., Leto, D., Chiang, S. H., Chang, L., & Saltiel, A. R. (2013). Inflammation produces catecholamine resistance in obesity via activation of PDE3B by the protein kinases IKKε and TBK1. *eLife*, 2, e01119. https://doi.org/10.7554/eLife. 01119
- Nakamura, J., Okamura, N., & Kawakami, Y. (2004). Augmentation of lipolysis in adipocytes from fed rats, but not from starved rats, by inhibition of rolipram-sensitive phosphodiesterase 4. Archives of Biochemistry and Biophysics, 425, 106–114. https://doi.org/10.1016/j.abb.2004.02.036
- Nikolaev, V. O., Bünemann, M., Hein, L., Hannawacker, A., & Lohse, M. J. (2004). Novel single chain cAMP sensors for receptor-induced signal propagation. The Journal of Biological Chemistry, 279(36), 37215– 37218. https://doi.org/10.1074/jbc.C400302200
- Omar, B., Zmuda-Trzebiatowska, E., Manganiello, V., Göransson, O., & Degerman, E. (2009). Regulation of AMP-activated protein kinase by cAMP in adipocytes: Roles for phosphodiesterases, protein kinase B, protein kinase a, Epac and lipolysis. *Cellular Signalling*, 21(5), 760–766. https://doi.org/10.1016/j.cellsig.2009.01.015
- Palmer, D., Jimmo, S. L., Raymond, D. R., Wilson, L. S., Carter, R. L., & Maurice, D. H. (2007). Protein kinase a phosphorylation of human phosphodiesterase 3B promotes 14–3-3 protein binding and inhibits phosphatase-catalyzed inactivation. *Journal of Biological Chemistry*, 282(13), 9411–9419. https://doi.org/10.1074/jbc.M606936200
- Perry, R. J., Camporez, J. G., Kursawe, R., Titchenell, P. M., Zhang, D., Perry, C. J., Jurczak, M. J., Abudukadier, A., Han, M. S., Zhang, X. M., Ruan, H. B., Yang, X., Caprio, S., Kaech, S. M., Sul, H. S., Birnbaum, M. J., Davis, R. J., Cline, G. W., Petersen, K. F., & Shulman, G. I. (2015). Hepatic acetyl CoA links adipose tissue inflammation to hepatic insulin resistance and type 2 diabetes. *Cell*, 160(4), 745–758. https://doi.org/10.1016/j.cell.2015.01.012

836. https://doi.org/10.1126/science.1074683

- Perry, S. J., Baillie, G. S., Kohout, T. A., McPhee, I., Magiera, M. M., Ang, K. L., Miller, W. E., McLean, A. J., Conti, M., Houslay, M. D., & Lefkowitz, R. J. (2002). Targeting of cyclic AMP degradation to beta 2-adrenergic receptors by beta-arrestins. *Science*, *298*(5594), 834–
- Petersen, M. C., Vatner, D. F., & Shulman, G. I. (2017). Regulation of hepatic glucose metabolism in health and disease. *Nature Reviews Endocrinology*, 13(10), 572–587. https://doi.org/10.1038/nrendo. 2017.80
- Rahn Landström, T., Mei, J., Karlsson, M., Manganiello, V., & Degerman, E. (2000). Down-regulation of cyclic-nucleotide phosphodiesterase 3B in 3T3-L1 adipocytes induced by tumour necrosis factor alpha and cAMP. The Biochemical Journal, 346(Pt 2), 337-343. https://doi.org/10.1042/bj3460337
- Richter, W., Day, P., Agrawal, R., Bruss, M. D., Granier, S., Wang, Y. L., Rasmussen, S. G., Horner, K., Wang, P., Lei, T., Patterson, A. J., Kobilka, B., & Conti, M. (2008). Signaling from beta1- and beta2-adrenergic receptors is defined by differential interactions with PDE4. The EMBO Journal, 27(2), 384–393. https://doi.org/10.1038/sj. emboi.7601968
- Robenek, H., Robenek, M. J., Buers, I., Lorkowski, S., Hofnagel, O., Troyer, D., & Severs, N. J. (2005). Lipid droplets gain PAT family proteins by interaction with specialized plasma membrane domains. *Journal of Biological Chemistry*, 280(28), 26330–26338. https://doi.org/10. 1074/jbc.M413312200
- Sancar, G., & Birkenfeld, A. L. (2024). The role of adipose tissue dysfunction in hepatic insulin resistance and T2D. *Journal of Endocrinology*, 262(3), e240115. https://doi.org/10.1530/JOE-24-0115
- Sancar, G., Liu, S., Gasser, E., Alvarez, J. G., Moutos, C., Kim, K., van Zutphen, T., Wang, Y., Huddy, T. F., Ross, B., Dai, Y., Zepeda, D., Collins, B., Tilley, E., Kolar, M. J., Yu, R. T., Atkins, A. R., van Dijk, T. H., Saghatelian, A., ... Evans, R. M. (2022). FGF1 and insulin control lipolysis by convergent pathways. *Cell Metabolism*, 34(1), 171–183. https:// doi.org/10.1016/j.cmet.2021.12.004
- Sárvári, A. K., Van Hauwaert, E. L., Markussen, L. K., Gammelmark, E., Marcher, A. B., Ebbesen, M. F., Nielsen, R., Brewer, J. R., Madsen, J. G. S., & Mandrup, S. (2021). Plasticity of epididymal adipose tissue in response to diet-induced obesity at single-nucleus resolution. *Cell Metabolism*, 33(2), 437–453. https://doi.org/10.1016/j.cmet. 2020.12.004
- Shakur, Y., Takeda, K., Kenan, Y., Yu, Z. X., Rena, G., Brandt, D., Houslay, M. D., Degerman, E., Ferrans, V. J., & Manganiello, V. C. (2000). Membrane localization of cyclic nucleotide phosphodiesterase 3 (PDE3). Two N-terminal domains are required for the efficient targeting to, and association of, PDE3 with endoplasmic reticulum. *Journal of Biological Chemistry*, 275(49), 38749–38761. https://doi.org/10.1074/jbc.M001734200
- Sharabi, K., Tavares, C. D., Rines, A. K., & Puigserver, P. (2015). Molecular pathophysiology of hepatic glucose production. *Molecular Aspects of Medicine*, 46, 21–33. https://doi.org/10.1016/j.mam.2015.09.003
- Shi, Q., Li, M., Mika, D., Fu, Q., Kim, S., Phan, J., Shen, A., Vandecasteele, G., & Xiang, Y. K. (2017). Heterologous desensitization of cardiac β-adrenergic signal via hormone-induced βAR/arrestin/PDE4 complexes. *Cardiovascular Research*, 113(6), 656–670. https://doi.org/10.1093/cvr/cvx036
- Snyder, P. B., Esselstyn, J. M., Loughney, K., Wolda, S. L., & Florio, V. A. (2005). The role of cyclic nucleotide phosphodiesterases in the regulation of adipocyte lipolysis. *Journal of Lipid Research*, 46(3), 494–503. https://doi.org/10.1194/jlr.M400362-JLR200

- Strålfors, P., & Honnor, R. C. (1989). Insulin-induced dephosphorylation of hormone-sensitive lipase. Correlation with lipolysis and cAMPdependent protein kinase activity. European Journal of Biochemistry, 182(2), 379–385. https://doi.org/10.1111/j.1432-1033.1989. th14842 x
- Surdo, N. C., Berrera, M., Koschinski, A., Brescia, M., Machado, M. R., Carr, C., Wright, P., Gorelik, J., Morotti, S., Grandi, E., Bers, D. M., Pantano, S., & Zaccolo, M. (2017). FRET biosensor uncovers cAMP nano-domains at β -adrenergic targets that dictate precise tuning of cardiac contractility. *Nature Communications*, 8, 15031. https://doi.org/10.1038/ncomms15031
- Tang, Y., Osawa, H., Onuma, H., Nishimiya, T., Ochi, M., & Makino, H. (1999). Improvement in insulin resistance and the restoration of reduced phosphodiesterase 3B gene expression by pioglitazone in adipose tissue of obese diabetic KKAy mice. *Diabetes*, 48(9), 1830–1835. https://doi.org/10.2337/diabetes.48.9.1830
- Team, R. C. (2024). R: A Language and Environment for Statistical Computing. In. Vienna, Austria.
- Terrin, A., Di Benedetto, G., Pertegato, V., Cheung, Y. F., Baillie, G., Lynch, M. J., Elvassore, N., Prinz, A., Herberg, F. W., Houslay, M. D., & Zaccolo, M. (2006). PGE(1) stimulation of HEK293 cells generates multiple contiguous domains with different [cAMP]: Role of compartmentalized phosphodiesterases. *The Journal of Cell Biology*, 175(3), 441–451. https://doi.org/10.1083/jcb.200605050
- Tuszynski, J. (2024). caTools: Tools: Moving Window Statistics, GIF, Base64. ROC AUC, etc. In.
- Van Liefde, I., Witzenburg, A., & Vauquelin, G. (1992). Multiple beta adrenergic receptor subclasses mediate the L-isoproterenol-induced lipolytic response in rat adipocytes. *Journal of Pharmacology and Experimental Therapeutics*, 262(2), 552–558. https://doi.org/10.1016/S0022-3565 (25)10793-3
- Wang, H., & Edens, N. K. (2007). mRNA expression and antilipolytic role of phosphodiesterase 4 in rat adipocytes in vitro. *Journal of Lipid Research*, 48(5), 1099–1107. https://doi.org/10.1194/jlr.M600519-JLR200
- Zacharias, D. A., Violin, J. D., Newton, A. C., & Tsien, R. Y. (2002). Partitioning of lipid-modified monomeric GFPs into membrane microdomains of live cells. *Science*, 296(5569), 913–916. https://doi.org/10.1126/science.1068539
- Zhang, J., Hupfeld, C. J., Taylor, S. S., Olefsky, J. M., & Tsien, R. Y. (2005). Insulin disrupts beta-adrenergic signalling to protein kinase a in adipocytes. *Nature*, 437(7058), 569–573. https://doi.org/10.1038/nature04140

SUPPORTING INFORMATION

Additional supporting information can be found online in the Supporting Information section at the end of this article.

How to cite this article: Krier, J., Spähn, D., Lopez, D. A. J., Nono, J. L., Seigner, J., Jacob, L., Ussar, S., Lukowski, R., Birkenfeld, A. L., & Sancar, G. (2025). PDE4D and PDE3B orchestrate distinct cAMP microdomains in 3T3-L1 adipocytes. *British Journal of Pharmacology*, 1–16. https://doi.org/10.1111/bph.70216